REPORT No. 405

APPLICATION OF PRACTICAL HYDRODYNAMICS TO AIRSHIP DESIGN

By RALPH H. UPSON and W. A. KLIKOFF

SUMMARY

The design of a large high-speed airship is primarily a structural problem, in which the most important stresses are those due, directly or indirectly, to aerodynamic forces on the surface of the hull. The force on any small element of the surface is most conveniently divided into two components, respectively tangent and normal to the surface. The tangent or skin-friction forces are so small per unit area that they are structurally almost negligible compared with the normal forces; yet their total integrated resultant is responsible for almost the entire drag of the hull, whereas the normal components of pressure are so nearly balanced over a good hull that their net resultant is practically zero. The interreaction of these very substantial forces is, of course, through the medium of stresses in the hull, and in combination with fin and inertia forces they are essential not only from a structural standpoint but also in the consideration of stability and control. The distribution of velocity and skin friction can also be indirectly determined from the normal force distribution. An accurate determination of the latter and its effects is therefore of the very first importance.

The pressure on ellipsoidal shapes is presented first in Part I as a foundation for more generalized formulas. Although any ellipsoid is susceptible of accurate mathematical treatment, only the case of a prolate spheroid with circular cross section is investigated here because of its approximation to airship hulls.

Part II deals with important adaptations of the ellipsoidal formulas, and other hydrodynamic relations to any airship hull, with particular reference to structural requirements.

In Part III the theoretical results are applied to the practical computation of airship stability, and relations established which can be evaluated from simple wind-tunnel tests.

In Part IV the same fundamentals are used in the determination of viscous forces, leading to an improved classification of airship drag, and a new outlook on drag generally.

Examples of practical airship characteristics are employed throughout.

INTRODUCTION

A determination of pressure distribution in a wind tunnel usually is tedious, expensive, and inaccurate. Even full-scale pressure readings have so far failed to give very consistent results, presumably due to local interference effects. Enough has been done experimentally, however, to show conclusively that the normal pressure is substantially unaffected by viscosity and skin friction except near the stern. The same conclusion is also reached from considering the above mentioned small magnitude of the unit tangential force. In most of the work the viscosity may therefore be ignored; and this is exactly the assumption on which the study of classical hydrodynamics has been based. This time-honored science, which for centuries was not much more than a mathematical toy, has thus found for itself at last a directly practical outlet in its increasing aeronautical use, particularly for lighter-than-air.

The aerodynamic forces on airship hulls have lately been investigated by different methods based on hydrodynamical theory of flow. Professor Von Karman (reference 5) has applied the method of sources and sinks combined with assumed vortices at the stern to the investigation of pressures on model of airship *Los Angeles*. Dr. R. Jones (reference 3) determined the pressure distribution on a prolate spheroid based on classical hydrodynamical theories. Dr. M. Munk (reference 2) by applying the theory of momentums has derived the resultant moment acting on the airship; and by assuming 2-dimensional transverse flow, has approximated the distribution of transverse force acting on airship hulls. Some of these investigations have been presented in complicated manner and some, by disregarding certain factors, lead to erroneous conclusions.

This paper, submitted at the request of the National Advisory Committee for Aeronautics, aims to overcome certain difficulties and to bring the subject generally up to date. The purpose of the first two parts is to present in concise shape all the formulas required for computation of the hydrodynamic forces, so that they can be easily computed for either straight or

curvilinear flight. Improved approximations are also introduced having a high degree of accuracy throughout the entire range of practical proportions. The remaining two parts of the report are devoted respectively to stability and skin friction, as functions of the same hydrodynamic forces.

SYMBOLS USED

P = any point on the surface,
P_0 = point at zero velocity,
ρ = density of air (standard = 0.00237 slugs),
μ = coefficient of viscosity,
V = velocity at point P (feet per second),
V_0 = velocity of hull relative to air at ∞ (feet per second),
p = pressure at point P (pounds per square foot),
$q = p_{max}$ = pressure at $P_0 = \frac{\rho}{2} V_0^2$ (pounds per square foot.)

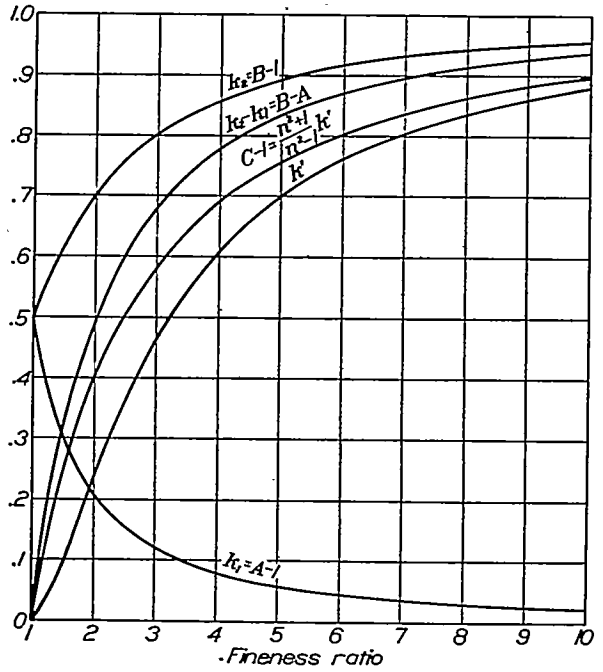

FIGURE 1.—Inertia coefficients of ellipsoids

Coefficients of additional mass of ellipsoids:

$$A = 1 + k_1 = \frac{e^3}{e - \frac{1}{2}\left(\frac{1}{n}\right)^2 \log \frac{1+e}{1-e}} = \frac{(n^2-1)^{3/2}}{n^2\sqrt{n^2-1} - n\log(n+\sqrt{n^2-1})}$$

where,

e = eccentricity of ellipse $= \frac{\sqrt{n^2-1}}{n}$,
n = fineness ratio $= a/b$,
a = major axis of ellipsoid,
b = minor axis of ellipsoid,
$B = 1 + k_2$, and is such quantity that $\frac{1}{2A} + \frac{1}{B} = 1$,

$$C = k' \frac{n^2+1}{n^2-1} + 1 = \frac{2A(n^2+1) - 6}{4An^2 - 3(n^2+1)},$$

k_1, k_2, and k' may be taken from tables of Lamb and Munk, for A, B, and C—see Table I and Figure 1,
θ = angle the direction of wind makes with axis (pitched flight),
ψ = angle the direction of wind makes with axis (yawed flight),
ψ_0 = angle the direction of wind makes with axis (circular flight)—(at center of volume),
α = angle the tangent at P makes with the major axis,
α_0 = angle the tangent at P_0 makes with the major axis,
ϕ = angle of arch between point P and a meridian perpendicular to the plane of the turning circle, or the horizontal meridian (equator) in case of pitched flight,
x, y = profile coordinates of the point P with center of ellipsoid taken as origin. (Fig. 2), x positive backward,
$r = y$ = radius of circular cross section at point P,
$V_0 = R\omega$ (for curved flight), where ω = angular velocity of ellipsoid (radians per second),
R = radius of circle in which center of volume moves (R = hull drag in Part IV),

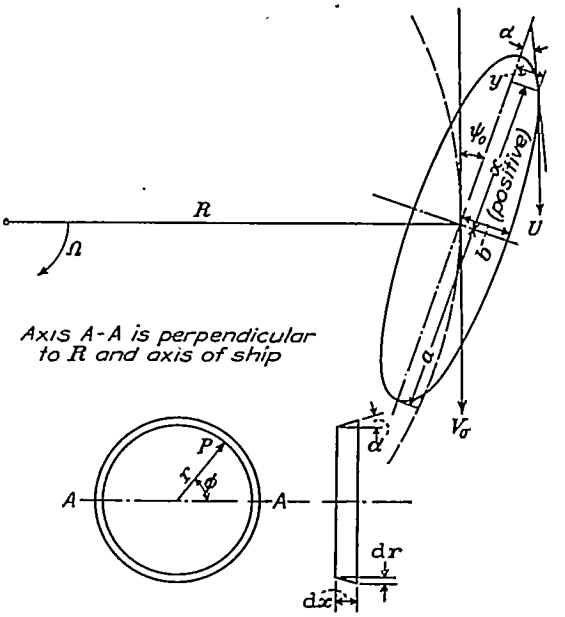

FIGURE 2.—Geometrical notation

S = cross section area of ellipsoid at point $P = \pi r^2$,
S_{max} = maximum cross section area of ellipsoid $= \pi b^2$,
dS/dx = rate of change of cross section $= 2\pi r \tan \alpha$,
vol = volume of the hull,
ΔF_T = transverse force per foot of axis,
ΔF_L = longitudinal force per foot of axis,
ΔM_L = longitudinal moment per foot of axis,
F_L = longitudinal force from bow to any station x,
$M = M_L + M_T$ = moment about station x of all forces forward of that point,
M_o = total turning moment about center of volume,
M_T = moment about station x of transverse forces forward of that point,
M_L = same, of longitudinal forces,
Q = transverse shear from bow back to any station x.

See Figure 10 for additional symbols applying to Part III.

REPORT No. 405

APPLICATION OF PRACTICAL HYDRODYNAMICS TO AIRSHIP DESIGN

PART I

HYDRODYNAMIC FORCES ACTING ON A PROLATE SPHEROID

For the fundamentals on which this study is based it is suggested that the references, particularly reference 1, be consulted. It is sufficient to state here that the velocity distribution assumes frictionless, incompressible, irrotational flow (whether the flight path is curved or straight), as given by Laplace's equation for velocity potential Φ. The pressure at any point P is then given by the expression:

$$\frac{p}{\rho}=\frac{\partial\Phi}{\partial t}-\frac{v^2}{2}$$

where v is the air velocity at P relative to undisturbed air. This is equivalent to an adaptation of Bernoulli's equation:

$$\frac{p}{\rho}=\frac{U^2}{2}-\frac{V^2}{2} \qquad \text{(ref. 3)}$$

where U is the free air velocity of point P ($=V_0$ for a point at radius R from center of turn), or for any point on the hull in straight flight.

NORMAL PRESSURE DISTRIBUTION

For curvilinear flight, the most general case (see reference 3), the pressure at any point can be algebraically expressed as:

$$\frac{p}{q}=\left(\cos\psi_0-\frac{r}{R}\sin\phi\right)^2+\left(\frac{x}{R}+\sin\psi_0\right)^2-\left\{A\cos\psi_0\cos\alpha+B\sin\psi_0\sin\alpha\sin\phi+[2S(C-1)-CS_{\max}]\frac{\cos\alpha\sin\phi}{\pi\ r\ R}\right\}^2-\left(B\sin\psi_0+\frac{xC}{R}\right)^2\cos^2\phi \qquad (1)$$

(See Pt. III for the relation between ψ_0 and R.)

In case the ellipsoid is moving straight at a certain angle of pitch θ, $R=\infty$, $\psi_0=\theta$, and the expression reduces to:

$$\frac{p}{q}=1-B^2\sin^2\theta\cos^2\phi-(A\cos\theta\cos\alpha+B\sin\theta\sin\alpha\sin\phi)^2$$

In case $\theta=0$, the expression for pressure at any point reduces to:

$$\frac{p}{q}=1-A^2\cos^2\alpha \text{ and } \frac{V_{\max}}{V_0}=A \qquad (2)$$

Point P_0, where velocity $=0$, and pressure is a maximum $\left(\frac{p}{q}=1\right)$ will be located where $\cot\alpha_0=\frac{B}{A}\tan\theta$.

At the point of minimum pressure where $\alpha=\frac{\pi}{2}-\alpha_0$

$$\frac{p_{\min}}{q}=1-A^2\cos^2\theta-B^2\sin^2\theta$$

$$=1-\frac{A^2\cos^2\theta}{\sin^2\alpha_0}=1-\frac{B^2\sin^2\theta}{\cos^2\alpha_0}$$

At point of zero pressure, where $V=V_0$

$$\frac{V^2_{\max}}{V_0^2}\sin^2(\alpha_0-\alpha)=1$$

when $\theta=0$, the zero pressure occurs at the point where

$$\cos\alpha=\frac{1}{A}$$

The pressure at any point for pitched flight in the plane of symmetry may also be expressed as:

$$\frac{p}{q}=1-\left(\frac{V}{V_0}\right)^2=1-\frac{V^2_{\max}}{V_0^2}\sin^2(\alpha_0-\alpha)$$

If we designate the side of ellipsoid turned to the flow as "windward," and the pressure at this side p_w; the side turned away from flow "leeward," and the pressure p_l; calling the meridian plane between the sides equatorial and expressing pressure on meridian plane p_e; then in case of pitched flight:

$$\frac{p_w}{q}=1-(A\cos\alpha\cos\theta+B\sin\alpha\sin\theta)^2 \qquad (3)$$

$$\frac{p_l}{q}=1-(A\cos\alpha\cos\theta-B\sin\alpha\sin\theta)^2 \qquad (3a)$$

$$\frac{p_e}{q}=1-B^2\sin^2\theta-A^2\cos^2\alpha\cos^2\theta \qquad (3b)$$

If the values of p_w, p_l, and p_e are plotted along the diameter of symmetry they do not lie on a straight line, except for a very elongated shape. (See fig. 3.)

At the equator the flow is at an angle ψ' to the meridian such that,

$$\tan\psi'=\frac{B\tan\theta}{A\cos\alpha}$$

and the resultant velocity ratio,

$$\frac{V^2}{V_0^2}=B^2\sin^2\theta+A^2\cos^2\alpha\cos^2\theta$$

INTEGRATED FORCES

Consider an element on the surface of an ellipsoid of revolution. The force due to aerodynamic pressure on a small arc per foot of axis will be $dF=pr\ d\ \phi$

This force can be subdivided into three components (fig. 2):

(*a*) Transverse, perpendicular to the axis AA.

$$dF_T=pr\sin\phi\ d\ \phi$$

(*b*) Longitudinal, parallel to the axis of ellipsoid.

$$dF_L=pr\tan\alpha\ d\ \phi$$

(*c*) Perpendicular to plane of symmetry, parallel to the axis AA; this component is evidently balanced by the component on the other side of the hull and is here disregarded.

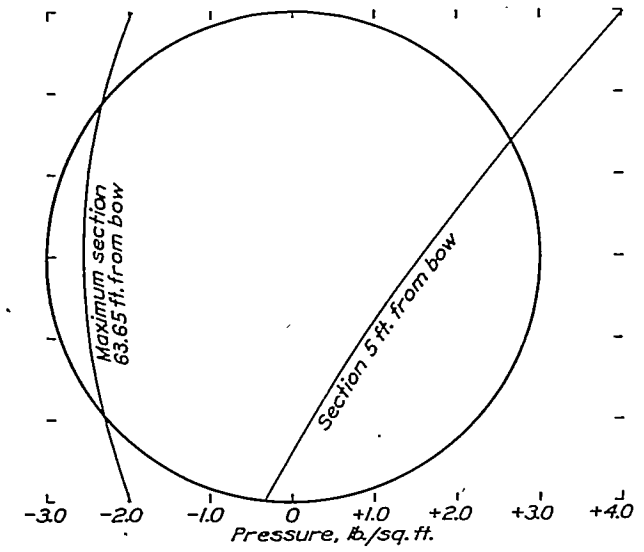

FIGURE 3.—Hydrodynamic pressure distribution over two cross sections—ZMC-2 plotted against the diameter of symmetry; $\theta=10°$, $v=50$ m. p. h.

The resultant transverse force per foot of axis on any section perpendicular to the axis, in case of circular flight is,

$$\frac{dQ}{dx}=\Delta F_T=2\int_{-\pi/2}^{\pi/2}pr\sin\phi d\phi=q\left\{AB\frac{dS}{dx}\sin\psi_0\right.$$
$$\left.-\frac{2}{R}\left[(2AC-2A+\sec^2\alpha)S-ACS_{max}\right]\right\}\cos^2\alpha\cos\psi_0 \quad (4)$$

In case of pitched flight,

$$R=\infty,$$

$$\psi_0=\theta,$$

and,

$$\Delta F_T=q\frac{AB}{2}\frac{dS}{dx}\cos^2\alpha\sin 2\theta=q\frac{AB}{2}\pi r\sin 2\theta\sin 2\alpha \quad (4a)$$

The longitudinal component of pressure produces a longitudinal force per foot of axis,

$$\Delta F_L=2\int_{-\pi/2}^{\pi/2}pr\tan\alpha d\phi.$$

In case of circular flight this evaluates to:

$$\Delta F_L=q\left\{2\cos^2\psi_0+2\left(\frac{x}{R}+\sin\psi_0\right)^2+\left(\frac{r}{R}\right)^2\right.$$
$$-2\left(A\cos\psi_0\cos\alpha\right)^2-\left(B\sin\psi_0+\frac{x}{R}C\right)^2-\left[B\sin\psi_0\sin\alpha\right.$$
$$\left.\left.+(2CS-CS_{max}-2S)\times\frac{\cos\alpha}{\pi rR}\right]^2\right\}\pi r\tan\alpha \quad (5)$$

In case of pitched flight the same expression reduces to:

$$\Delta F_L=q\left\{2-2A^2\cos^2\theta\cos^2\alpha\right.$$
$$\left.-B^2(1+\sin^2\alpha)\sin^2\theta\right\}\pi r\tan\alpha \quad (5a)$$

In case of straight flight at $\theta=0$,

$$\Delta F_L=2q\left(1-A^2\cos^2\alpha\right)\pi r\tan\alpha=p\frac{dS}{dx} \quad (6)$$

The effect of this force, although often disregarded in the present design of airships will undoubtedly be considered with increase of speed.

The longitudinal force per foot of axis if integrated over the length of ellipsoid will give the total longitudinal aerodynamic force to any section. If integrated over the whole length of the hull it will be equal to:

$$F_L=2q\left(k_2\right)\left(\frac{\text{vol}}{R}\right)\sin\psi_0,$$

in case of circular flight. In case of pitched flight it will return to zero at the end.

The total longitudinal force will reach its maximum compressive value a short distance behind the bow. At the maximum section it has a slight negative (tension) value, which in case of straight flight of the ellipsoid ($\theta=0$) is,

$$F_L=qS_{max}\left[1-A^2\frac{n^2}{n^2-1}\left(1-2\frac{\log n}{n^2-1}\right)\right]$$

The expression of transverse force if integrated either graphically or mathematically over the length of ellipsoid from the bow to any station x produces the curve of aerodynamic shear. At the maximum section the shear reaches the value:

$$Q=q\frac{AB}{2}S_{max}\frac{n^2}{n^2-1}\left(1-2\frac{\log n}{n^2-1}\right)$$
$$\sin 2\psi_0-2q\frac{(\text{vol})}{R}k_1\cos\psi_0$$

By integrating the shear curve over the total length the expression for aerodynamic moment around the stern due to transverse force can be obtained.

$$M_T = q\,(k_2 - k_1)\,(\text{vol})\,\frac{n^2}{n^2-1}\sin 2\psi_0 - 2qa\,\frac{(\text{vol})}{R}\,k_1\cos\psi_0$$

The last two expressions for shear and transverse moment are derived for the case of circular flight; in case of pitched flight ($\psi_0 = \theta$), the last terms of these equations will evidently be equal to zero.

The longitudinal component of pressure, neglected in some of the recent investigations, produces a reverse moment, $dM_L = r \sin\phi\ dF_L = pr^2 \tan\alpha \sin\phi\ d\phi = r \tan\alpha\ dF_T$.

Then the longitudinal moment per foot of axis,

$$\Delta M_L = 2\int_{-\pi/2}^{\pi/2} r \tan\alpha\ dF_T = -r\Delta\ F_T \tan\alpha$$

This moment will always have a sign opposite to the sign of transverse shear. If integrated over the length of the ellipsoid for either pitched or curved flight, it produces a total longitudinal moment,

$$M_L = q(k_2 - k_1)\,\frac{(\text{vol})}{(n^2-1)}\sin 2\,\psi_0.$$

Combining this moment with the transverse moment, the expression for total turning moment around the stern to which the ship is subjected,

$$M = q(k_2 - k_1)\,(\text{vol})\sin 2\,\psi_0 - 2\,q\,k_1\,(\text{vol})\,\frac{a}{R}\cos\psi_0.$$

If the moment is taken around the center of volume, the last term disappears, making the total moment for either circular or pitched flight:

$$M_0 = q(k_2 - k_1)\,(\text{vol})\sin 2\,\psi_0. \qquad (7)$$

This agrees with the expression derived by Doctor Munk in his consideration of general flow around airship hulls. (Reference 2.) In his other work Doctor Munk has disregarded the effect of longitudinal components of pressure and, as will be shown, his expression for transverse force is needlessly inexact.

The fundamental difference between the circular and pitched flight in an ideal fluid is that in case of pitched flight there are no resultant transverse or longitudinal forces; while in case of circular flight there is a net transverse force component:

$$F_T = 2q(k_1)\,(\text{vol})\,\frac{\cos\psi_0}{R} \qquad (8)$$

and also a net longitudinal force component:

$$F_L = 2q(k_2)\,(\text{vol})\,\frac{\sin\psi_0}{R} \qquad (9)$$

The two components have a resultant passing through the center of flight path curvature, thus satisfying the total energy conditions.

It will be interesting to note that some of the aerodynamic loads may be expressed as functions of "windward," "leeward," and "equatorial" pressures which were previously discussed, e. g.,

$$\Delta F_T = \pi\,\frac{r}{2}\,(p_w - p_l)$$

$$\Delta F_L = \pi\,\frac{r}{2}\,(p_w + p_l + 2p_e)$$

$$\Delta M_L = \pi\,\frac{r^2}{2}\,(p_l - p_w)\tan\alpha$$

The above expressions are theoretically correct for circular as well as pitched flight.

REPORT No. 405

APPLICATION OF PRACTICAL HYDRODYNAMICS TO AIRSHIP DESIGN

PART II

APPROXIMATION OF HYDRODYNAMIC FORCES ON AIRSHIP HULLS

A critical study of the mathematical formulas applying to true ellipsoids throws considerable light on the effect of other curves.

It may be observed that all the pressures and integrated forces are functions of the radius of cross section and the slopes at the particular point, and of general nondimensional coefficients of additional mass. Furthermore, there is a direct connection between these characteristics. Thus, for ellipsoids, it may be shown that

$$A=\frac{2a}{\int_{-a}^{a}\cos^2\alpha\,dx}$$

We now proceed to apply the expressions derived for an ellipsoidal shape to any airship hull. Several methods can be used for this purpose.

Equivalent ellipsoids.—As the bows of many airships approach or are actually sections of ellipsoids (ZMC–2, R–101), these may be computed as ellipsoids and a modified curve can then be drawn for the stern of the ship. This method is recommended by Doctor Cox (reference 8), and will be discussed with the transverse stern force distribution.

Another method for shapes departing more from the ellipsoid is to determine the additional mass coefficients for the complete hull and use them as constants in the ellipsoidal formulas, determining the actual airship forces from known characteristics of the airship curve (radius and slope). For the determination of additional mass coefficients three simple methods of figuring equivalent ellipsoids may be used:

1. Actual $n=\frac{L}{D}$
2. By length $n=\sqrt{\frac{\pi L^3}{6\ (\text{vol})}}$
3. By diameter $n=\frac{6\ (\text{vol})}{\pi D^3}$

The truth will usually be best expressed by the formula which gives the lowest result. Fine pointed shapes, for example, take the last formula, because the extreme point of the tail simply adds to the geometrical length without appreciably affecting the aerodynamic characteristics. The effective value of n is also decreased by the dissymmetry between the bow and stern profiles, but not as far as would be obtained by assuming the bow profile at both ends.

A still more general, but still approximate method, is to fit at any point on the hull profile an ellipsoidal element, which would reproduce all the hydrodynamic characteristics at that point. This ellipsoidal element will, as far as possible, have the same geometric characteristics as the point on the curve, but tentatively, may be a part of an ellipsoid whose over-all dimensions do not correspond at all to the hull profile, i. e., its additional mass coefficients may be entirely different from the hull shape. The application of these equivalent ellipsoids may be checked by applying the general hydrodynamic proposition for frictionless, nonviscous fluid that integration of axial and transverse pressure components over the surface of any streamline shape must equal zero for uniform straight motion. This method will be more particularly applied to the determination of transverse force to be described later.

The pressure distribution plotted according to this method is shown on Figure 4, curve 1. This curve was plotted assuming the equivalent ellipsoid fitted to any point on the hull to have the following characteristics relative to the original hull curve:

1. Concentric about longitudinal axis,
2. Maximum diameter equal, ($D=2b_e$),
3. Vertical ordinates at the point equal, ($r=y_e$),
4. Product of first and second derivatives of the curves at the point equal,

which lead to the following relation between the fineness ratio of an equivalent ellipsoid and the characteristics of the point on the hull curve:

$$n_e^3=\frac{D^2}{4r^4}\left(\frac{\sqrt{(D/2)^2-r^2}}{\tan\alpha\left(\frac{d^2r}{dx^2}\right)}\right)$$

PRESSURE DISTRIBUTION BY SOURCE INTENSITY

For still greater accuracy we must go back to more fundamental relations. The method of determining a stream-line form from a predetermined source and sink line is not new and was used in Naval Architecture and Airship Design. (References 4 and 6.) It was expected

that the forms of low resistance could be determined by this method and that these forms would have an advantage that, knowing the hull profile and the intensity of sources and sinks, the pressure distribution could be easily found. In most cases, however, a predetermined distribution of sources and sinks does not give a profile curve with any simple mathematical equation that can be conveniently manipulated. Therefore, in practice it seems preferable to predetermine the profile curve and find the source distribution to correspond, though recognizing the greater initial labor involved.

For determination of the sink and source line shown on Figure 4, Taylor's method (reference 6) was used, except that the problem was the reverse one of plotting the curve of source and sink intensity for a known body. This was done by means of the equation (for any one transverse section):

$$V\pi y=\frac{1}{2}\int_0^{l} f(\Sigma)\left(1+\frac{x-\Sigma}{\sqrt{(x-\Sigma)^2-y^2}}\right)\mathrm{d}\Sigma$$

Where $f(\Sigma)$, the source intensity, varies as a function of x (here called Σ to distinguish it from the abscissa of the section under investigation), and is integrated over the length of the hull in each case.

Thus a complete series of equations was derived, all these equations being interconnected by the known equation of the hull curve. The method was first checked by reproducing a full ellipsoid having known characteristics. The same procedure was then applied to the actual airship hull.

These equations after being solved for $f(\Sigma)$, reproduced the sink and source line corresponding to the hull shape. Knowing $f(\Sigma)$ values, the horizontal velocity at the point was determined by the equation,

$$V_h=\frac{1}{2}\int_0^{e}(f\Sigma)\frac{(x-\Sigma)}{[(x-\Sigma)^2+y^2]^{3/2}}\mathrm{d}\Sigma$$

then the final velocity at the point,

$$V=\frac{V_0+V_h}{\cos\alpha}$$

This value of the velocity was used in the pressure equation,

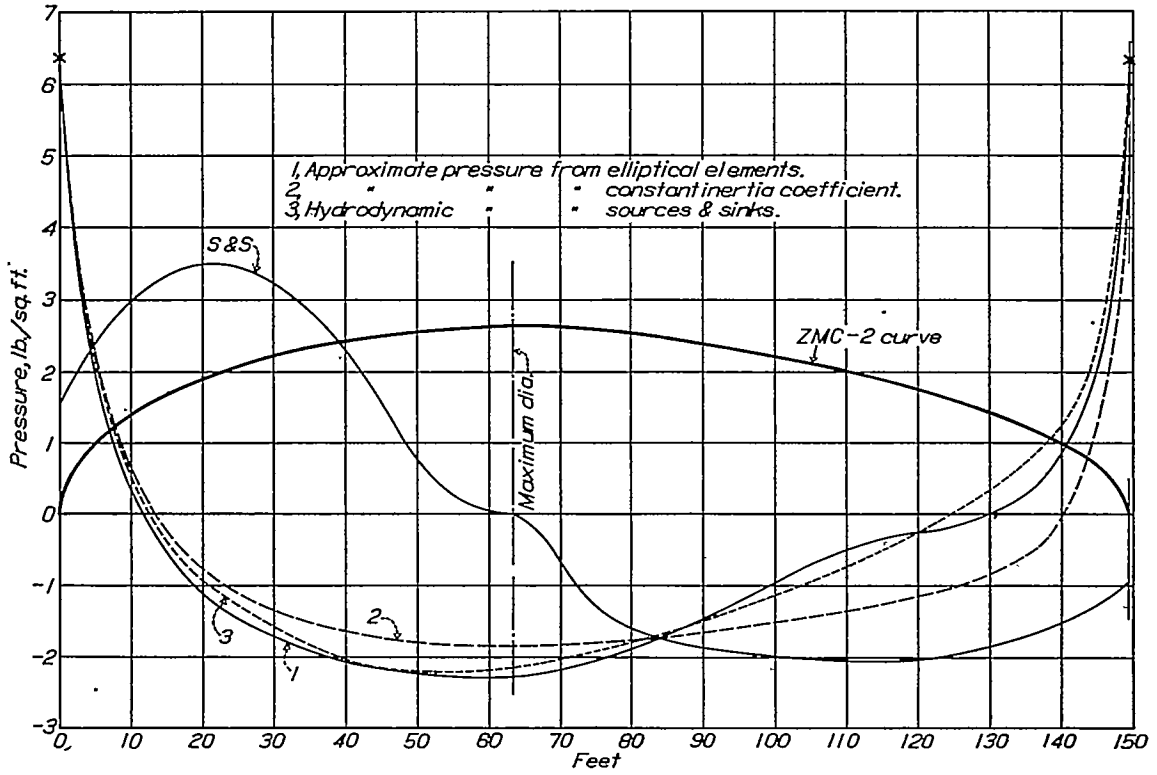

FIGURE 4.—Comparison of pressure curve derived from sink and source line (S & S) with curve obtained by fitting ellipsoids. $\theta=0°$, $v=50$ m. p. h., *ZMC-2* shape, EH curve with E stern

$$\frac{p}{q}=1-\left(\frac{V}{V_0}\right)^2$$

for determination of the pressure at a given point.

Von Karman (reference 5) made an independent investigation of pressure distribution using a sink and source line to determine the flow in a longitudinal plane, and a system of double sources to determine the flow in a transverse plane. By writing general expressions for the flow, he determined the values of the velocity components in both planes, due to each system of flow separately. Knowing the values of these velocities, the pressure was determined by Bernoulli's equation.

The pressure distribution curves based on ellipsoidal formulas for straight flight are plotted in Figure 4 for the metal-clad *ZMC-2* hull: (1) by the method of fitting ellipsoids to points on the hull; (2) by applying the mass coefficients of the complete hull to equation (2); for comparison (3), the actual hydrodynamic pressure distribution by the method of sources and sinks is also shown in the same figure.

TRANSVERSE FORCE IN PITCHED FLIGHT

The main difficulty in applying ellipsoidal elements lies in the approximation of additional mass coefficients to fit not only the point where the forces are investigated, but also to fit the complete hull.

In this connection an interesting observation was made that the product of inertia coefficients $A \times B$ for

$$\Delta F_T = q \frac{dS}{dx} \cos^2 \alpha \sin 2\theta = q\pi r \sin 2\theta \sin 2\alpha \quad (10)$$

The above simple, single formula is all that is necessary for plotting this most important aerodynamic force with a high degree of accuracy as to general distribution and magnitude. (Fig. 5.) After this force is plotted it will be found, due to the above approximation, that the positive force over the bow and negative force over the stern do not balance exactly. From a quantitative standpoint this discrepancy is unimportant, but if further analysis is required on the basis of an ideal fluid, it may be desirable to have an exact balance. This can be easily done, at the same time making the force curve at the bow a still closer approximation, by simply moving the whole curve

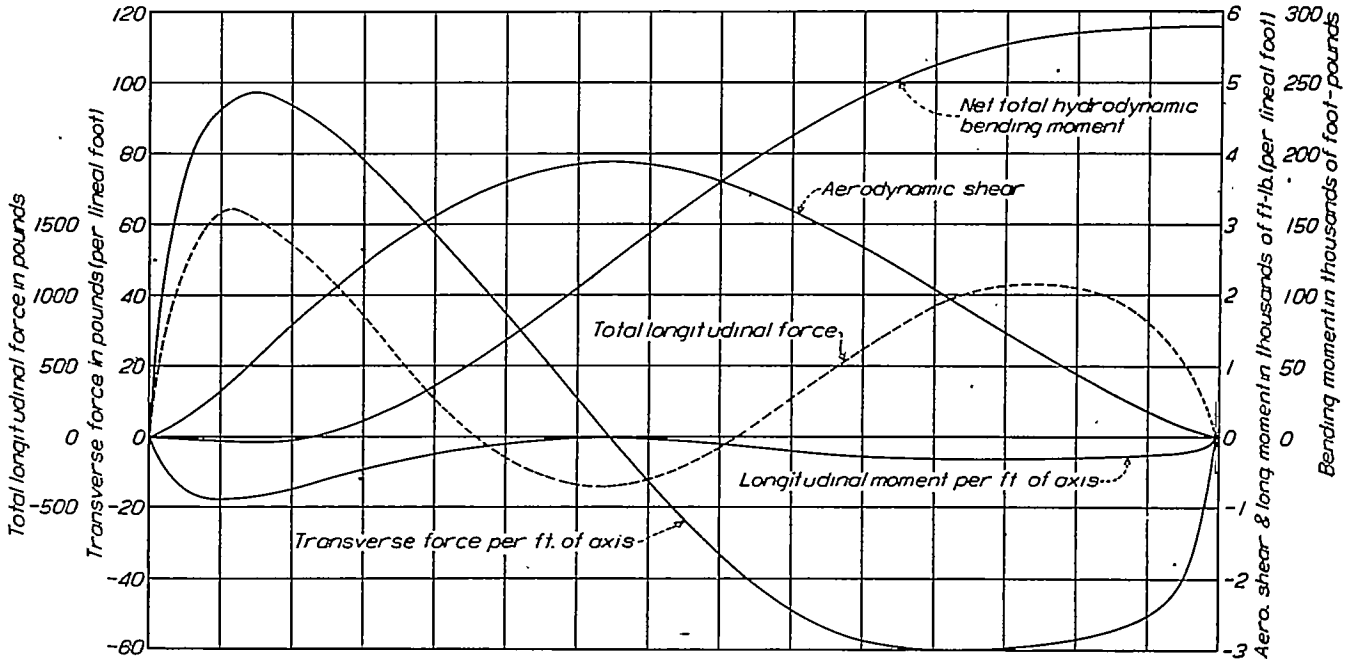

FIGURE 5.—Hydrodynamic loads, shears, and moments—*ZMC-2* hull. EH curve with E stern, $\theta = 10°$, $v = 50$ m. p. h. Total longitudinal force computed for $\theta = 0°$

all usable fineness ratios is practically equal to two, as is shown in Table I.

Returning to the ellipsoidal formulas, it will be noticed that the mass coefficients are represented exclusively by the factor $\frac{AB}{2}$ in the expression (4a) for transverse force per foot of axis. Thus for ellipsoidal type of flow the point characteristics (i. e., ordinate and slope) of any sectional element determine the transverse force almost independently of characteristics elsewhere. We may assume that the same holds true for a series of gradually varying elements and hence for the hull curve itself.

It would thus appear that the factor $\frac{AB}{2}$ can be neglected, for most practical purposes, over the entire range of usable fineness ratios. The general formula for transverse force in pitched flight may then be written,

bodily up or down enough to make the positive and negative areas balance.

The close approximation of the lateral force derived by the above method to the force measured by wind tunnel tests can be seen from Figures 6, 7, and 8, showing the distribution of transverse force on modern airship hulls.

Von Karman (reference 5), extending his investigation of pressure distribution to determination of transverse forces has arrived at the following expression,

$$\Delta F_T = \rho \pi r (u_x w_x + u_r w_r).$$

Where u and w are the velocities due to the longitudinal and transverse motion, respectively, the subletters x and r refer to the respective longitudinal and radial components at a point in the plane of symmetry.

Applying this expression to ellipsoidal analysis, we get,

$$u_x w_x + u_r w_r = \frac{AB}{4} V_0^2 \sin 2\alpha \sin 2\theta \qquad \text{or,}$$

approximately, $= \frac{V_0^2}{2} \sin 2\alpha \sin 2\theta$ (the same result).

AERODYNAMIC SHEAR IN PITCHED FLIGHT

After the curve of transverse force is plotted, it can be graphically integrated by means of a planimeter and the curve derived will represent the aerodynamic shear Q to any point, in pitched flight. The maximum shear, at a point where $\Delta F_T = 0$, may be approximated by a similar method to what was used for transverse force, thus:

$$Q_{max} = q\sqrt{B-A}\, S_{max} \sin 2\theta$$

where,

$$\sqrt{B-A} = \sqrt{k_2 - k_1}$$

is the mean effective value using apparent mass coefficients for the entire hull.

LONGITUDINAL MOMENT IN PITCHED FLIGHT (PER FOOT OF AXIS)

As was mentioned for ellipsoids, the longitudinal moment per foot of axis,

$$\Delta M_L = -\Delta F_T\, r \tan \alpha$$

Knowing therefore the value of ΔF_T and the geometrical characteristics of the point, the expression for longitudinal moment can be easily plotted. The longitudinal moment should have a negative sign over the entire length of hull.

NET AERODYNAMIC MOMENT IN PITCHED FLIGHT

The net moment to any point will be the algebraic sum or difference of the areas under the shear and longitudinal moment curves. This assumes temporarily that the hull is held as a cantilever at the stern, the moment reaching a maximum at this point. (Fig. 5.) The net value of moment curve ordinate at the stern represents the total hydrodynamic turning moment on the hull, and must satisfy the equation (7).

$$M = q\,(k_2 - k_1)\,(\text{vol}) \sin 2\theta$$

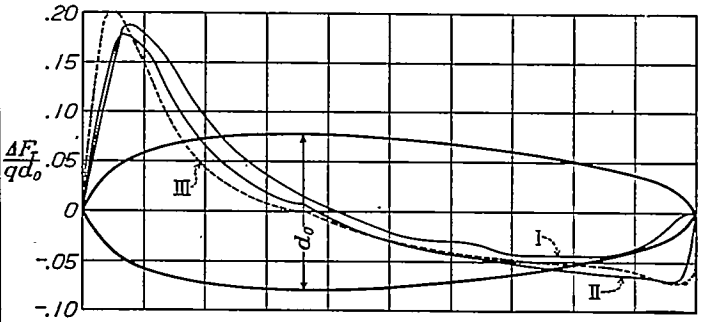

FIGURE 6.—Transverse force on model RS-1 ($\theta = 9°$). I. Transverse force from wind tunnel tests by Bureau of Standards (Technical Data Files, McCook Field, D527/RS-1). II $= \Delta F_T = q \times \frac{dS}{dX} \times \sin 2\theta \cos^2 \alpha$ (corrected for hydrodynamic balance.) III $= \Delta F_T = q \times \frac{dS}{dX} (k_2 - k_1) \times \sin 2\theta$ Munk's formula $(k_2 - k_1) = 0.78$

TRANSVERSE STERN FORCE

The plotting of hydrodynamic forces, shears, and moments does not correspond to actual conditions observed on the airship hull. It will be noticed that in an ideal fluid no resultant force occurs, and the airship is subjected only to the action of a couple, whose magnitude equals the hydrodynamic moment. Actually, the area under the distributed transverse force curve at the stern is considerably smaller than at the bow, producing a resultant force at the bow in the direction of inclination of the ship's axis. (Figs. 6, 7, and 8.) Superimposed on the hydrodynamic flow at the stern there is evidently an airfoil type of flow in a direction opposite to the ship's inclination, producing vortices as is the case with an airplane wing.

Doctor Von Karman (reference 5) has computed the magnitude of these vortices and has arrived at results closely approaching the actual load conditions.

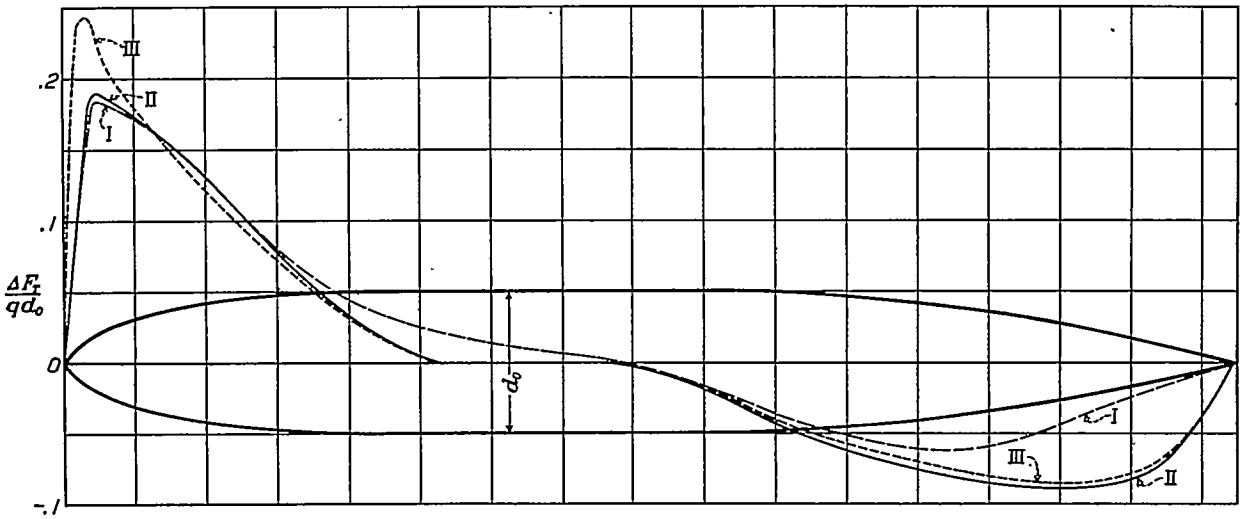

FIGURE 7.—Transverse force on model R-33 ($\theta = 10°$). I. Transverse force from wind tunnel tests (A. R. C.; R & M No. 801); II $= \Delta F_T = q \times \frac{dS}{dX} \times \sin 2\theta \cos^2 \alpha$; III $= \Delta F_T = q \frac{dS}{dX} (k_2 - k_1) \sin 2\theta$ Munk's formula $(k_2 - k_1 = .924)$

The following method, somewhat approaching that recommended by Doctor Cox (reference 8), can be more conveniently used. In this case it is desirable to obtain from wind tunnel tests at high Reynolds Number the resultant force and moment on the bare airship hull under conditions similar to those analyzed. When these values are not available, they can be approximated from results of tests of airship models of shapes similar to the one analyzed. The curve of hydrodynamic transverse force can be then modified at the stern in such manner that its area would be reduced by the amount equal to the force determined in the wind tunnel. The shape of the curve should be modified to approach the curves of transverse force as determined in wind tunnels on hulls of similar general characteristics. This distribution of transverse force will then approach very closely to the actual conditions, and if the forces at the control surfaces and the inertia or other balancing forces are also considered, the complete load diagram can be reproduced.

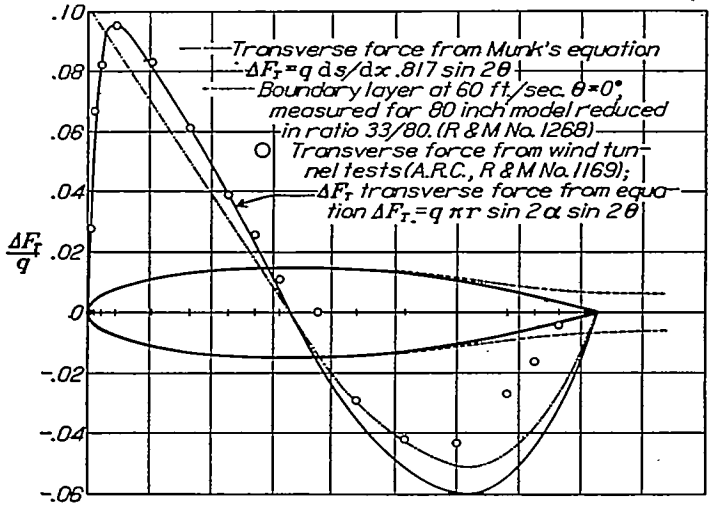

FIGURE 8.—Transverse force on model R-101 ($\theta = 10°$). Scale of model=one-quarter; length of model=33.01 inches

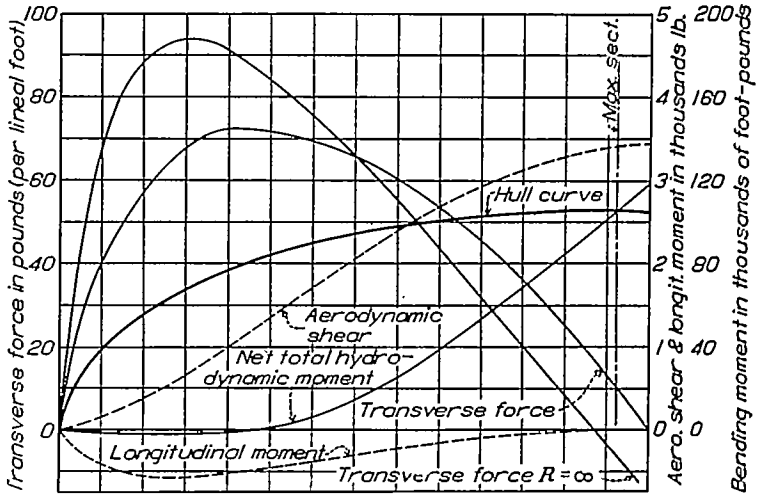

FIGURE 9.—Circular flight. Hydrodynamic loads, shears, and moments—Bow *ZMC-2* ($\psi = 10°$, $v = 50$ m. p. h., $R = 600$ feet)

CIRCULAR FLIGHT

For the determination of forces in circular flight, the exact ellipsoidal expressions should be used, making approximation for the additional mass coefficients as outlined above. The distribution of transverse force over the bow for circular flight of the *ZMC-2* is shown in Figure 9. This distribution is plotted for the same speed, with the angle of yaw at *c. g.* the same as in the pitched flight investigation. It can easily be observed that the transverse force is smaller in the case of circular flight than in the corresponding case of pitched flight. Considering also that the transverse force in circular flight is balanced by inertia force largely distributed over the hull, while the force in pitched flight may be largely balanced by excess of weight concentrated at the points of load application, it can clearly be seen that pitched flight will produce higher shears and moments than circular flight for otherwise similar conditions. Therefore, the investigation of pitched flight alone will usually serve as a guide for the determination of the longitudinal strength of airships, although circular flight should also be at least tentatively investigated, if there are any doubts as to the strength in this plane. The relation between R and ψ_0 in actual flight and their effect on stability is treated in Part III.

CONCLUSION

The investigation of the possibility of applying the hydrodynamic ellipsoidal formulas to airship hulls leads to the conclusion that these formulas can be divided into two groups: (1) Formulas which can be approximated to permit the determination of flow characteristics from geometrical properties of the individual point at which the flow is desired, and (2) formulas which include the general shape as a whole.

The formulas which include only the geometrical point characteristics, such as the formula for transverse force in pitched flight, leading to the determination of shear and bending moment, can be applied to any airship hull, and for the most part are probably even more accurate than the results of actual tests.

The formulas for pressure distribution and for longitudinal force in the case of pitched flight, and for all the aerodynamic forces in case of circular flight, are dependent on characteristics of the point and also on the hull shape as a whole. In this case the designer should be careful in choosing the coefficients of additional mass corresponding to the designed hull. If these are properly applied results very closely approaching those of true hydrodynamic flow can be obtained.

In regard to the stern force, it should be noted that the hull force in the immediate neighborhood of the fins, particularly between and behind them, is further modified by the presence of the fins themselves. It is proposed to deal with this more particularly in a subsequent report on fin design.

REPORT No. 405

APPLICATION OF PRACTICAL HYDRODYNAMICS TO AIRSHIP DESIGN

PART III

AIRSHIP STABILITY

The consideration of airship stability in yaw is based on the principle that any tendency of the airship to yaw from its path may be considered as the tendency to swing into a circular path deviating from the original direction. The study of stability in yaw therefore simplifies itself to a study of the airship in circular flight and a consideration of the transverse forces and moments acting on it.

In this connection it should be first noted that for motion of the airship deviating from the straight path the angle of attack is no longer fixed but will vary throughout the length of the airship, reaching the highest values at the stern. The wind-tunnel tests give only the moments at a constant angle of attack throughout the hull; but as the principal stabilizing forces on the airship act at the stern, the wind tunne results may be utilized providing proper allowance is made for the above-mentioned variation of yaw angle in actual flight. This may be done by the use of hydrodynamic principles.

Consider an airship of mass $m = \rho \times \text{vol}$, traveling on a circular path, with angle of yaw $= \psi_0$ (relative to undisturbed air); velocity tangential to path $= V_0$ and radius $= R$ (all taken at the center of volume). The center of gravity is assumed to be coincident with the center of volume. k_1 and k_2 are additional mass coefficients of the airship, A and B the total virtual mass coefficients. (Fig. 10.)

The airship is assumed to be subjected to the following forces:

1. Transverse component of centrifugal force due to the mass of the ship itself $= \frac{mV_0^2}{R} \cos \psi_0$ distributed through the hull, with resultant acting at center of volume.

2. Transverse component of virtual centrifugal force due to the additional mass of air set in motion around the hull $= \frac{mV_0^2}{R} k_1 \cos \psi_0$ which appears as aerodynamic pressure with resultant applied at center of volume. This is equivalent to the ellipsoidal equation (8), but may also be derived from a more general consideration of momentum. (Reference 2.)

3. Distributed aerodynamic force which does not produce any resultant force but produces an unbalancing moment, $M_0 = \frac{mV_0^2}{2} (k_2 - k_1) \sin 2 \psi_0$; from equation (7).

4. Stern force acting at a distance l from the center of gravity, whose magnitude to balance the above moment should be $\frac{mV_0^2}{2l} (k_2 - k_1) \sin 2 \psi_0$.

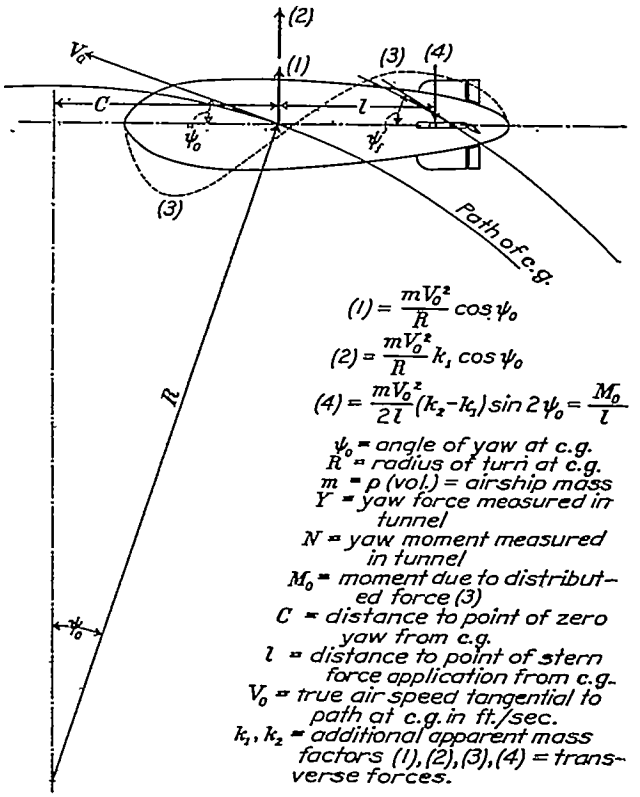

FIGURE 10.—Transverse forces on airship hull in circular flight

Relation between turning radius and angle of yaw.—As long as the airship is in a condition of steady turn, the forces should balance or, from the above,

$$\frac{mV_0^2}{R} (1 + k_1) \cos \psi_0 = \frac{mV_0^2}{2l} (k_2 - k_1) \sin 2 \psi_0. \quad (11)$$

thus,

$$\frac{(1 + k_1)}{R} = \frac{(k_2 - k_1)}{l} \sin \psi_0$$

$$\frac{A}{R} = \frac{B - A}{l} \sin \psi_0$$

from which,

$$R=\frac{(1+k_1)}{(k_2-k_1)}\frac{l}{\sin\psi_0}\approx\frac{(1+k_1)}{(k_2-k_1)}\frac{l}{\psi_0}57.3=\frac{57.3\,Al}{\psi_0(B-A)} \quad (12)$$

(ψ_0 in degrees).

It may be noticed that the angle of yaw of any one point on the axis is a linear function of distance along the axis. Thus as ψ_0 is the angle of yaw at the *c. g.*, let c be the distance forward of *c. g.* to point where the local angle of yaw is zero. Then,

$$c=R\sin\psi_0=\frac{Al}{B-A}$$

If ψ_f is the local angle of yaw at the point of application of the stern force (l feet behind the *c. g.*),

$$\tan\psi_f=\frac{c+l}{c}\tan\psi_0=\frac{B}{A}\tan\psi_0$$

or,

$$\psi_f\approx\frac{B}{A}\psi_0 \quad (13)$$

from which we get as an alternative value of the turning radius,

$$R=\frac{57.3\,Bl}{\psi_f(B-A)} \quad (12a)$$

The above considerations of an airship in a perfect fluid in a condition of neutral stability are only approximated in practice, due to the distributed nature of the tail force, as already noted. In the case of a bare hull at a fixed angle of pitch or yaw, the distributed hydrodynamic force at the stern is reduced while the distributed force at the bow remains the same. Usually this difference is termed "dynamic lift on bare hull" of the airship. Its real center of action is, of course, forward of the *c. g.* For the purpose of the above analysis, however, it is considered not in the sense of a resultant force at the bow of the airship, but as a force at the stern acting in a direction to oppose the theoretical turning moment M_o which would otherwise apply in the analysis of a perfect fluid. This force is the Y_h force which is measurable in wind-tunnel tests on a bare hull for a certain angle of yaw ψ or pitch θ. Its moment arm about the *c. g.* as measured in the wind tunnel is,

$$l_h=\frac{M_o'-N_h}{Y_h}.$$

When the fin surfaces are introduced they produce a force Y_f and moment $Y_f l_f$. For the purpose of analysis we here assume $l_h=l_f=l$ combining Y_h and Y_f into a single force Y, which is not far from actual results.

An experimental check is found in a comparison of the radius of turn computed from formula (12) with that obtained in full scale tests. In the case of the *Los Angeles* the computed radii are 4 per cent off from the experimental, but are closer to the experimental values than the results derived by the hydrodynamically inexact formula used in N. A. C. A. Technical Report No. 333. The full scale tests on the *C-7* (N. A. C. A. Technical Report No. 208) are within 2.3 per cent of the computed figure. A somewhat larger discrepancy in the case of the *ZMC-2* will be considered later in connection with the car effect.

Stability criteria.—Comparing actual flight with the theoretical, where the forces were in balance, it can be seen that if the actual force at the stern is larger than the theoretical stern force opposing the turning movement, the airship will tend to return from the circular to its original straight path.

Whether this condition is fulfilled may now be determined from a simple static wind-tunnel test, preferably at high Reynolds Number. The only further assumption involved is that the stern force for a given airship speed is determined by the angle of yaw *at* the fins, regardless of what it is elsewhere. As will be shown later, this seems to be almost exact for the fin force proper and usually a fair approximation for the balance of the stern force. Thus, for stability computation, the wind-tunnel angle ψ must now be taken as equivalent to ψ_f, not to ψ_o, because from (13)

$$\psi_o=\frac{A}{B}\psi_f=\frac{A}{B}\psi \quad (13a)$$

Referring back to the condition for neutral stability, equation (11) for small angles can now be written:

$$\frac{mV_o^2}{R}A=\frac{mV_o^2A}{lB}(B-A)\frac{\psi}{57.3}$$

of which the first term is the actual centrifugal force, including that of the additional air mass, and the second term is the balancing stern force necessary to hold a constant radius of turn. If Y exceeds this force we have positive stability. Generally speaking then, we may define the degree or criterion of stability as the ratio of the actual stern force to the balancing stern force. Then any value greater than unity is stable. Thus we get stability criterion No. 1:

$$S.\,C._Y=\frac{28.6lYB}{q(\text{vol})A(B-A)\psi} \quad (14)$$

The same method of reasoning can be also applied to moments. The moment measured in the tunnel for a certain angle of yaw will be evidently:

$$N=M_o'-Y_hl_h-Y_fl_f$$

The moment due to the stern force alone is evidently,

$$=M_o'-N=Y_hl_h+Y_fl_f\approx Yl \quad (15)$$

This moment should be larger than the theoretical moment to have the ship stable, or

$$(M_o'-N)>mV_0^2\,(B-A)\frac{A}{B}\frac{\psi}{57.3}$$

Taking the ratio as before, we get stability criterion No. 2:

$$S.\ C._N = \frac{B}{A}\left(1 - \frac{28.6\ N}{q\ \text{vol}\ (B-A)\ \psi}\right) \qquad (16)$$

A third stability criterion may be based on an experimental determination of the resisting yawing moment by the use of damping apparatus or a whirling arm. It seems obvious, however, that additional mechanical complications of this kind are not justified unless they serve to reproduce more closely the type of motion found in actual flight. For example, the oscillating type of damping apparatus would seem to be particularly futile. Though any method by which the stern force or moment can be plotted against the local angle of attack at the stern gives a means of approximating the required ratio, the most important test condition is high Reynolds Number.

The evaluation of a damping test is best expressed as a moment N_D around the *c. g.* (computed from the test moment around the actual center used) for a given transverse component of stern speed v_f at the position l behind the *c. g.* Then $\frac{v_f}{V_o}$ corresponds to ψ_f (in radians), and we get as stability criterion No. 3:

$$S.\ C._D = \frac{B}{A}\left(1 - \frac{N_D}{\rho V_0\ \text{vol}\ (B-A)\ v_f}\right) \qquad (17)$$

Tail arm length.—Proper use of the formula for $S.\ C._Y$ depends on getting the correct value for l. The fin arm l_f may be taken as the distance from the *c. g.* of the ship back to the mean *c. p.* of the fins, the latter point for any one fin being found as follows: Find the centroid of the entire fin, including control surface; draw a line through the centroid, in the plane of the fin, parallel to the hull meridian at the front of the fin; from where this line cuts the leading edge, measure back along the same line one-fourth of its length from leading edge to trailing edge. For most models l can be taken as approximately equal to l_f but is more accurately given by the expression:

$$l = \frac{M_o' - N}{Y} = \frac{1}{Y}\left(\frac{q}{28.6}\ \text{vol}\ (B-A)\psi - N\right) \qquad (18)$$

In case this gives a value differing much from l_f, the bare hull force and tail arm, Y_h and l_h may be similarly determined from a test without the fins, and the figures checked by equation (15). In special cases portions of the hull force may be considered quite separately from the fin force, in a similar manner to the car force, now to be considered.

Effect of car.—It is clear that an additional fin force at the center of gravity, such as due to a car, will serve to carry part of the centrifugal force. For a given angle of yaw it will cause the ship to turn on a smaller radius, which in turn will produce a larger local angle at the fins, thus improving the stability. Another, less precise way, of explaining it is to say that there is a relative damping moment between the car and the fins which opposes a tendency to turn. The important thing to note here is that the above two statements are not of two different effects, but refer to one and the same effect.

Though the more general case of a plurality of side forces at different points on the hull may be solved by a similar method, there seems to be no practical importance in trying to express the result in a single algebraic formula. Hence, we return to the case of a side force at the *c. g.* In this case, let Y_c be the difference in transversive force with car on and off, measured at an angle of ψ in the tunnel. Then by the principles already laid down, the actual car force in free flight will be $\frac{Y_c\,\psi_0}{\psi}$ for an angle of ψ at the fins. The balance of forces for equilibrium is:

$$\frac{mV_0^2 A}{R} \approx \frac{Y_c\,\psi_0}{\psi} + \frac{M_0}{l} \qquad (19)$$

where,

$$M_0 = mV_0^2 (B-A)\frac{\psi_0}{57.3}$$

and,

$$R = \frac{57.3\,l}{\psi - \psi_0}$$

From (19) we get,

$$\frac{\psi}{\psi_0} = \frac{28.6 Y_c l}{q\ \text{vol}\ A\ \psi} + \frac{B}{A}$$

which can be substituted in the expression for R. For a wind tunnel moment N, we have the second stability requirement as before:

$$M - N > mV_0^2\ (B-A)\frac{\psi_0}{57.3} \qquad (20)$$

which, expressed as a ratio in terms of ψ is:

$$S.\ C._{N'} = \left(\frac{B}{A} + \frac{28.6\ Y_c l}{q\ \text{vol}\ A\ \psi}\right)\left[1 - \frac{28.6\ N}{q\ \text{vol}\ (B-A)\ \psi}\right] \qquad (21)$$

Thus, aside from interference effects, the stability is slightly improved by a fin force at the *c. g.* Even further forward, there is not likely to be much negative effect, due to approaching the point of zero yaw. Put more broadly, it is on the safe side to consider any distributed load as concentrated at the point of application of its resultant.

A word of warning here: measure N with the car (or cars) on, to be sure of catching any blanketing of the fins so caused. If Y is the stern force, S. C. $_{N'}$ is derived from equation (20) by putting $M - N = Yl$ and substituting for ψ_0 in terms of ψ.

Pressure and velocity distribution.—Having determined the free flight connection between ψ_0, ψ and R we may substitute either way in equation (1), Part I. A practical example is plotted in Figure 9. Expressed in terms of the stern angle ψ, where $x = l$ by means of equations (12a) and (13a), we have a convenient means of checking the validity of the assumptions on which the stability criteria are based.

The particular question here is whether there is enough difference, in the hitherto unconsidered flow pattern, as between turning and simple yaw to make a serious difference in the resulting stern force for a given value of ψ. Taking the extreme condition of a fin element subjected to the full theoretical flow at the hull surface, its actual reaction, compared to the free air value, is increased in the ratio,

$$F' = \frac{V^2}{V_0^2}\frac{\psi'}{\psi}$$

where, ψ' is the angle between the streamline and the meridian at the point in question. But for small angles (in radians),

$$\psi' = \sin \psi' = \frac{V_c}{V}$$

or,

$$F' \approx \frac{VV_c}{V_0^2\psi} \approx \frac{V_m V_c}{V_0^2\psi}$$

where V_m is the meridian component and V_c the circumferential component of V.

Equation (1), by its derivation, consists of four main terms of which the first two are the component terms of $\frac{V^2}{V_0^2}$ the third is $\frac{V_m^2}{V_0^2}$ and the fourth is $\frac{V_c^2}{V_0^2}$. For the position of maximum fin effectiveness $\phi = 0$; also putting $\sin \psi_0 = \psi_0$ (radians), $\cos \psi_0 = 1$ and substituting for R, ψ_0 and x as above we get,

$$F' = A\left(A + C - \frac{AC}{B}\right)\cos \alpha$$

Referring now to Table I or to Figure 1, it may be seen that the factor $A\left(A + C - \frac{AC}{B}\right)$ takes a value of 2.25 for $n = 1$, 2.0 for $n = \infty$, and 1.94 for $n = 5$, or is practically equal to 2 for the entire range of usable fineness ratios.

Applying similar approximations to equation (3b) for simple yaw ($\theta = \psi$), we get as the factor of increase,

$$F = AB \cos \alpha \approx 2 \cos \alpha \approx F'$$

Therefore, within the range of hydrodynamic conditions, the fin force at small angles is close to a straight line function of ψ for either curved flight or simple yaw, as originally assumed. The boundary layer and other modifications of flow, probably of small effect in relation to the present subject matter, will be taken up in a later report.

Limitation of assumptions.—It should be noted finally that the assumed straight line variation of the hull and fin forces with yaw angle is modified for the hydrodynamic forces when ψ becomes so large that the relation,

$$\sin 2\psi = 2 \sin \psi = 2\psi$$

no longer holds within the desired order of accuracy. And the assumption for the fin force breaks down entirely at the burble point of the fin airfoils. This is particularly noticeable for fins of high aspect ratio, such as used on the *ZMC-2*, this ship showing a very definite tendency to "spin" in an extreme turn.

Conclusions.—For most purposes, equations (14) and (16) are recommended, giving greatest credence to the one giving the lowest value of *S. C.* and designing so as to make it at least 1.0 and preferably 1.15. Serious discrepancies between the two criteria should, however, be investigated for effects of distributed force, interference, and burbling. The angle is preferably taken as half of the algebraic difference between equal positive and negative angles, not more than $\pm 10°$, Y and N being similarly derived. For larger angles, substitute $\frac{dY}{d\psi}$ for $\frac{Y}{\psi}$ and $\frac{dN}{d\psi}$ for $\frac{N}{\psi}$ plotting the values of *S. C.* against ψ.

Stability in pitch may be analyzed in exactly the same way, the principal difference being the negligible effect of the cars, and the static righting moment due to the vertical distance between the center of volume and the *c. g.* For the latter reason there is seldom any difficulty about the stability in pitch if that in yaw is satisfactory.

The *ZMC-2*, designed by these methods, indicated a slightly positive stability at small angles, a result well substantiated in practice. Examples of unstable airships were the *Shenandoah*, and the Army *AC*. There is no question about the latter by results from either wind tunnel or actual flight. The *Shenandoah*, however, although admittedly unstable in flight, did not seem to have as bad a reputation as its low criterion would indicate. Its very long and generally poor shape gives a distribution of transverse hull force sufficient to be a substantial factor. But even taking this into account the criterion is still quite low. Hence, it seems probable that the results of experience with the airship were largely colored by the large radius of turn, and by the time element contributed by the large moment of inertia involved in any unstable deflection from the straight path. In this case the principal danger of an unstable condition remains in its effect of magnifying the forces due to a sudden gust. Thus a sound and careful analysis of stability is of the utmost importance, particularly in the case of large airships where the result from a control standpoint is likely to be masked by elements involved in the size as such.

In any case the establishing of stability is but a preliminary to the determination of actual forces for specific conditions of flight.

REPORT No. 405

APPLICATION OF PRACTICAL HYDRODYNAMICS TO AIRSHIP DESIGN

PART IV

FRICTIONAL FORCES

Here we determine the approximate distribution and magnitude of the frictional drag on a large airship hull. Analysis will proceed on the following assumptions:

1. Turbulent type of boundary layer, of negligible thickness compared to the hull dimensions.
2. Flow otherwise frictionless and irrotational.
3. Distribution of unit tangential force proportional to the square of the local air velocity relative to the surface.
4. Magnitude of the total integrated force determined with reference to the mean effective Reynolds Number of the hull as a whole.
5. Axial motion of an ellipsoidal hull.

Force and energy relations.—Let dR_0 be the horizontal component of skin friction resistance on a circular element of surface of axial dimension dx. In the preliminary analysis we assume that this force varies exactly as the area, and as the square of the air velocity. Therefore, we may write, $dR_0 = C\rho\pi y V^2\,dx$, where C is a coefficient, and ρ is the density in slugs. From the ellipse equation, $y=\frac{1}{n}\sqrt{a^2-x^2}$, by hydrodynamics, Eq. (2)

$$V^2 = A^2V_0^2\cos^2\alpha = \frac{A^2V_0^2(a^2-x^2)}{a^2-x^2\left(1-\frac{1}{n^2}\right)}$$

Then, for the entire ellipsoid,

$$R_0 = 2C\pi\rho\int_0^a yV^2dx = \frac{2C\rho\pi A^2V_0^2}{n}\int_0^a\frac{(a^2-x^2)^{3/2}}{a^2-x^2\left(1-\frac{1}{n^2}\right)}dx$$

where V_0 is the speed of the ship (feet per second) and A is the hydrodynamic relation, $\frac{V_{max}}{V_0}=1+k_1$. By integration between the prescribed limits,

$$R_0=\frac{\pi^2}{2}C\rho A^2V_0^2a^2\frac{n+2}{(n+1)^2} \qquad (1)$$

With the proper value of C, to be determined, the above equation gives the integrated axial force contributed by the skin friction. That it is not the total drag due to the skin friction may now be made apparent by energy considerations.

Let dE be the energy per unit time absorbed by the same circular element of surface, along the meridian increment ds. Then if dF is the force along ds (integrated around the circle);

$$dE = VdF = C\rho\pi yV^3\frac{dx}{\cos\alpha} \qquad (2)$$

but,

$$V^3 = A^3V_0^3\cos^3\alpha = \frac{A^3V_0^3(a^2-x^2)\cos\alpha}{a^2-x^2\left(1-\frac{1}{n^2}\right)}$$

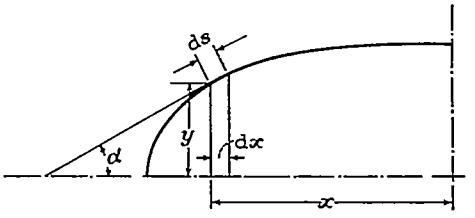

FIGURE 11

Substituting and integrating as before,

$$E=\frac{\pi^2}{2}C\rho A^3V_0^3a^2\frac{n+2}{(n+1)^2}$$

But if the total drag is R, $E=V_0R$, and,

$$R=\frac{\pi^2}{2}C\rho A^3V_0^2a^2\frac{n+2}{(n+1)^2} \qquad (3)$$

or,

$$\frac{R}{R_0}=A=1+k_1$$

In other words, the skin friction drag R_0 must be increased by a "pressure drag" of k_1R_0 to get the total drag R due directly to the viscous forces. This strongly discredits the opinion sometimes advanced (as a result of unreliable tests at low Reynolds Number) that it is possible to get a negative pressure drag. It also makes the direct viscous drag of airships (and boats) quite sensitive to changes of form as well as to changes of surface area and ship speed.

True viscous force.—To get an idea of the magnitude of force involved, C must now be evaluated,

taking into account the errors already introduced by the preliminary assumptions as to the exponents of the length and velocity. Using the formula of Diehl ("Engineering Aerodynamics," and N. A. C. A. Technical Note No. 102),

$$C=C_F=0.0375\ (6{,}350\times V_eL)^{-0.15}=\frac{0.01}{(V_eL)^{0.15}} \qquad (4)$$

(for standard sea-level conditions); where L may be taken as the axial length of the hull, rather than the meridian length, to allow for the end taper; or,

$$L=2a$$

V_e is the mean effective velocity, which may be evaluated as follows:

Referring to equation (3), this may be written in the form,

$$R=C\frac{\rho}{2}SV_e^2 \qquad (3')$$

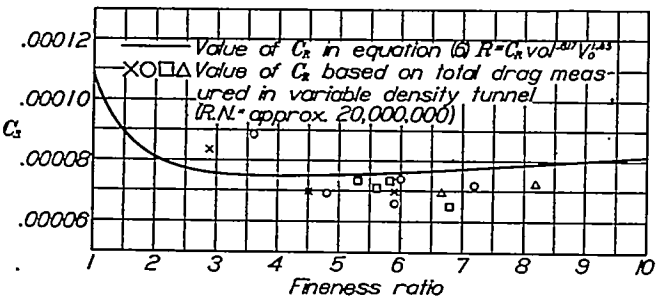

FIGURE 12.—Variation of resistance with fineness ratio

in which the surface area,

$$S=K_s\,a\,b$$

K_s being a geometrical coefficient varying from 12.0 for $n=2$ to 11.4 for $n=8$. From equations (3) and (3') we then have,

$$R=C\frac{\rho}{2}a\,b\,K_s\,V_e^2=C\frac{\rho}{2}a^2\,\pi^2\,A^3\,V_e^2\frac{n+2}{(n+1)^2}$$

from which,

$$V_e^2=\frac{\pi^2A^3n\ (n+2)\ V_0^2}{K_s\ (n+1)^2}$$

Substituting in (4),

$$C=0.0077\ \frac{K_s^{0.075}\ (n+1)^{0.15}}{a^{0.15}\ A^{0.225}\ n^{0.075}\ (n+2)^{0.075}\ V_0^{0.15}} \qquad (5)$$

and from (3),

$$R=0.00011\ A^{2.775}\ a^{1.85}\ V_0^{1.85}\ \frac{(n+2)^{0.925}}{n^{0.075}\ (n+1)^{1.85}}$$

(for $\rho=0.00238$ and $K_s=11.7$)

In terms of the volume $\left(=\frac{4\ \pi\ a^3}{3n^2}\right)$,

$$C=\frac{(n+1)^{0.15}}{100A^{0.225}\ \mathrm{vol}^{0.05}\ n^{0.175}\ (n+2)^{0.075}\ V_0^{0.15}} \qquad (5')$$

and,

$$R=\frac{A^{2.775}\ n^{1.158}\ (n+2)^{0.925}\ \mathrm{vol}^{0.617}\ V_0^{1.85}}{22{,}000\ (n+1)^{1.85}} \qquad (6)$$

For practical use this can be simplified to

$$R=C_R\ \mathrm{vol}^{0.617}\ V_0^{1.85} \qquad (6')$$

where C_R is a coefficient involving A and n (A also depending on n) which is plotted on the attached chart (fig. 12) for various values of n.

Discussion of results.—An interesting fact about the curve is that the minimum drag is shown at a fineness ratio greater than what would cause any great amount of burbling over a properly shaped hull. Thus the fineness ratio for minimum drag is apparently determined mainly by frictional forces alone. A supplementary indication is that practically minimum frictional drag, for a given volume, may be attained with any fineness ratio between about 3 and 6. But naturally the proper hull curve to prevent burbling becomes increasingly important for the lower fineness ratios; and with a ratio much under 4 a considerable amount of burbling must apparently be reckoned with at the best. In line with modern boundary layer theory, it appears further that this burbling at the lower fineness ratios is indirectly due to the sharp increase of energy loss from viscous friction, particularly around the maximum section.

The magnitude of the axial skin friction component around any one section, per unit axial length, is given by,

$$\frac{dR_0}{dx}=2CqA^2y\pi\ \cos^2\alpha \qquad (7)$$

where C has the value given in equation (5). The approximation here involved in assuming C constant over a long hull makes the calculated value of $\frac{dR_0}{dx}$ a little too low at the bow and too high at the stern. Greater accuracy in respect to the actual force distribution will depend on further research into the detailed structure and growth of the boundary layer.

Equations (6') and (7) are in a form which can be applied to any fair hull shape by estimating the equivalent ellipsoid, discussed in Part II.

A similar method may be followed in dealing with other problems involving the boundary layer, including cases of inclined and curvilinear flight.

It should be noted that there is still some question about the exact coefficient and exponent of the Reynolds Number. For smooth surfaces the coefficient as here used is more likely to be high than low. For the exponent, Von Karman uses -0.2 instead of -0.15 (with a coefficient to correspond), but the bulk of the evidence seems to favor the exponent here used. (See reference 12.)

Additional light on this point may be had from the values for various model tests in the variable density

wind tunnel as plotted in Figure 12. These are on the basis of C_R in equation (6′), all at a Reynolds Number of about 2×10^7. It will be noted that most of them fall below the theoretical curve; and most of them also show less variation with Reynolds Number than predicted from theory. An offhand conclusion might be that the exponent and coefficient both need revision. However, data collected by B. M. Jones (reference 12), shows quite clearly that the laminar type of flow is still often an appreciable element at the Reynolds Number of 10^7, but probably would not be so at full scale values of 10^8 and over. In other words, these test results are probably not yet out of the transition stage, and hence do not quite comply with the first assumption on which this study was based. An experimental check of this supposition might be had from observing the change due to an artifiical increase of turbulence in the same tunnel. Lacking evidence to the contrary, it seems to be another case of the theoretical result being on the whole more reliable and practical than the direct experiment; although in this case the extrapolation of several of the test results leads almost exactly to the theoretical value for full scale conditions.

In the computation of the parasite drag of outside parts the proper coefficient and exponent will, of course, depend on the character of the part in question. If the true local velocity V (instead of V_0) is used, however, and the result further increased by the energy factor $\frac{V}{V_0}$ much of the additional drag at low fineness ratios, commonly attributed to interference, will be found accounted for.

End conditions.—It remains finally to consider the instructive end conditions presented by the two extremes of fineness ratio, 0 and ∞.

In the first case of $n=0$, a circular disk normal to the flow, it can be shown that $K_S=\frac{2\pi}{n}$ and $A=\frac{2}{\pi n}$, while L may be assumed equal to b (the radius). Substituting the corresponding value of C in equation (1) gives for the direct skin friction:

$R_0=$ (a finite coefficient)$\times n^{0.075}\ b^{1.85}\ V_0^{1.85}=0$. This is not surprising in view of the fact that cos α is everywhere zero except at the extreme edge. But as energy is taken from the air, the drag can not be zero. On the energy basis, therefore, the viscous drag, here entirely in the form of "pressure drag," is,

$$R=AR_0=\infty$$

a result involving flow dimensions obviously out of line with the original assumptions on which it is based, and hence inapplicable to a practical case.

In the case of $n=\infty$, $K_S=\pi^2$, $A=1.0$, and by a similar process,

$$R=R_0=0.00011ba^{0.85}\ V_0^{1.85}$$
$$=0.01\ Sq\ (LV)^{-0.15}$$

which leads back, as it should, to the basic skin friction formula.

CONCLUSIONS

In conclusion of this part of the report, it is recommended for practical analysis that airship drag be divided into the following parts:

1. Viscous hull drag, of which the proportion $\frac{1}{A}$ appears as skin friction proper, the balance as pressure drag.
2. Burbling hull drag, creating an unknown proportion of pressure drag, usually positive, and a negative (relative to Item 1) skin friction drag. This item as a whole is probably always positive for practical hull shapes, but vanishingly small for the larger fineness ratios.
3. Parasite drag of adjacent parts, considered as acted upon by the actual air flow locally in which they are placed. (See discussion above.)
4. Interference effect, of the same parasite parts, on the hull drag (mostly modifying Item 2).

Item 1 is obtained for full scale by formula (6′) (the coefficient and exponents being subject to possible future refinement); or, for a model with unknown type of flow, by subtracting the axial resultant of the measured pressure distribution from the total measured drag and multiplying the remainder by A.

Item 3 is obtained by wind tunnel test or computation corrected to speeds obtained by formula or estimate.

The sum of Items 1 and 2 is obtained from a large or high-density tunnel, with maximum turbulence in the air flow.

The sum of Items 1, 2, 3, and 4 is similarly obtained; and can also be had from actual flight tests.

If C_R is used as a coefficient of total drag, it has the following relation to the shape coefficient C_S:

$$\text{Drag}=C_S\ q\ \text{vol}^{2/3}=C_R\left(\frac{\rho}{\rho_0}\right)^{0.85}\left(\frac{\mu}{\mu_0}\right)^{0.15}\text{vol.}^{0.617}\ V_0^{1.85}$$

where ρ_0 and μ_0 are the standard density and viscosity, respectively.

June 1, 1931.

REFERENCES

1. Lamb, H.: Hydrodynamics. Cambridge, Fourth Edition, 1916.
2. Munk, M.: Fundamentals of Fluid Dynamics for Aircraft Designers. The Ronald Press, 1929. Note on the Pressure Distribution Over the Hull of Elongated Airships with Circular Cross Section. T. N. No. 192, N. A. C. A., 1924. Remarks on the Pressure Distribution Over the Surface of an Ellipsoid Moving Translationally Through a Perfect Fluid. T. N. No. 196, N. A. C. A., 1924.

3. Jones, R.: The Distribution of Normal Pressures on a Prolate Spheroid. R. & M. No. 1061, British A. R. C., 1925.
4. Prandtl, L.: Applications of Modern Hydrodynamics to Aeronautics. T. R. No. 116, N. A. C. A., 1921.
5. Von Karman, Theodor: Calculation of Pressure Distribution on Airship Hulls. T. M. No. 574, N. A. C. A., 1930.
6. Taylor, D. W.: Ship-Shaped Stream Forms. Transactions of Institute of Naval Architects, 1894.
7. Jones, R., and Williams, D. H.: The Distribution Pressure Over the Surface of Airship Model U. 721 Together with a Comparison with the Pressure Over a Spheroid. R. & M. No. 600, British A. C. A., 1919.
8. Cox, H. R.: The External Forces on an Airship Structure with Special Reference to the Requirements of Rigid Airship Design. Royal Aeronautical Society, September, 1929.
9. Burgess, C. P.: Airship Design. Ronald Press, 1927.
10. Diehl, W. S.: Engineering Aerodynamics. Ronald Press, 1928.
11. Ower, E., and Hutton, C. T.: Investigation of the Boundary Layers and the Drags of Two Streamline Bodies. R. & M. No. 1271, British A. R. C., 1929.
12. Jones, B. M.: Skin Friction and the Drag of Streamline Bodies. R. & M. No. 1199, British A. R. C., 1928.

TABLE I

INERTIA COEFFICIENTS OF ELLIPSOIDS

$n=\frac{a}{b}$	$A=\frac{}{1+k_1}$	$B=\frac{}{1+k_2}$	$C=\frac{}{1+k'\ \frac{n^2+1}{n^2-1}}$	$B-A=\frac{}{k_2-k_1}$	$A\times B$
1.0	1.5	1.5	1.0	0	2.25
1.5	1.305	1.621	1.244	.316	2.115
2.0	1.209	1.702	1.400	.493	2.058
2.5	1.156	1.763	1.505	.607	2.038
3.0	1.122	1.803	1.582	.681	2.023
4.0	1.082	1.860	1.689	.778	2.013
5.0	1.059	1.895	1.760	.836	2.007
6.0	1.045	1.918	1.807	.873	2.004
7.0	1.036	1.933	1.839	.897	2.003
8.0	1.029	1.945	1.867	.916	2.001
9.0	1.024	1.954	1.887	.930	2.001
10.0	1.021	1.960	1.901	.939	2.001
∞	1.000	2.000	2.000	1.000	2.000